

Sensor and Simulation Notes

Note 247

29 December 1978

CLEARED
FOR PUBLIC RELEASE

PL/PA 5/19/97

ELECTROMAGNETIC CONSIDERATIONS
OF A SPATIAL MODAL FILTER FOR SUPPRESSION
OF NON-TEM MODES IN THE TRANSMISSION-LINE TYPE
OF EMP SIMULATORS

D.V. Giri
LuTech, Inc., Berkeley, CA

Carl E. Baum
Air Force Weapons Laboratory
and

Hagen Schilling
NBC Research and Development Institute
of the Federal Armed Forces
Federal Republic of Germany

ABSTRACT

The subject of this note is the suppression or damping of non-TEM modes in the transmission-line type of EMP simulator. This suppression may be accomplished by introducing a spatial modal filter (SMF), initially in the output conical section of the simulator. In this note, we deal with the electromagnetic considerations of the SMF which is essentially decoupled from the principal TEM mode. Although these considerations, in general, apply to any wave guiding structure (open or closed) that can support a dominant TEM mode, attention is currently being focused on the two-parallel-plate transmission-line type of EMP simulator.

PL 96-1257

ELECTROMAGNETIC CONSIDERATIONS
OF A SPATIAL MODAL FILTER FOR SUPPRESSION
OF NON-TEM MODES IN THE TRANSMISSION-LINE TYPE
OF EMP SIMULATORS

ABSTRACT

The subject of this note is the suppression or damping of non-TEM modes in the transmission-line type of EMP simulator. This suppression may be accomplished by introducing a spatial modal filter (SMF), initially in the output conical section of the simulator. In this note, we deal with the electromagnetic considerations of the SMF which is essentially decoupled from the principal TEM mode. Although these considerations, in general, apply to any wave guiding structure (open or closed) that can support a dominant TEM mode, attention is currently being focused on the two-parallel-plate transmission-line type of EMP simulator.

Acknowledgement

We are thankful to Mr. Bill Kehrer for his encouragement and interest in this problem. For many useful discussions, tanks are also due Dr. F. M. Tesche.

I. INTRODUCTION

An important class of EMP simulators is the parallel-plate transmission-line type. This type of an electromagnetic structure is essentially an open waveguide, between the conductors of which a transient pulse with a planar wavefront must travel. In practice, however, the fields obtained in the working volume can depart from the ideal TEM behavior owing to the excitation and propagation of non-TEM modes. It has been known for some time [1 to 5] that a finitely wide parallel-plate transmission line can support and propagate TE and TM modes if they are excited for any reason. Since the chief object of such an EMP simulator is to produce an EMP environment appropriate to a plane wave (outside the source region), it is desirable to suppress the non-TEM modes without disturbing the TEM wave. To successfully accomplish this suppression, a clear understanding of the characteristics of the TEM and non-TEM (i.e., TE and TM) modes is essential. Much detailed work has been done concerning the TEM properties of both the parallel-plate [6 to 9] and the conical [10, 11] transmission lines. References [12,13] have considered the conical transmission line as a launcher and receptor of waves on the cylindrical transmission line by introducing the concept of dispersion distances, or equivalently, dispersion times. Formulas have also been developed [13] for the TEM mode coefficient in terms of the cross-section fields. Detailed calculations of TE and TM modes of propagation are currently available for the two limiting cases of narrow (separation \gg width) [1] and wide (separation \ll width) [4,5] plates. A parametric study is presently in progress [14] for the general case where the separation to width ratio is not restricted. This study will consider geometries of the existing (ALECS

and ARES) and future (ATLAS I and II) transmission-line type of EMP simulator facilities at the Air Force Weapons Laboratory, as well as the laboratory model simulator at Harvard University. Comparisons of the electromagnetic field calculations from this study with the available experimentally measured fields in ALECS and Harvard's model simulator is expected to lead to an identification of the effects of the higher order modes. In any case, there exists a need for suppressing or damping the non-TEM modes.

In Section II, the departure of the measured fields in the working volume from the ideal TEM behavior will be considered, and in Section III, available computations of TE and TM modes in the parallel-plate region will be reviewed. Sections IV and V deal with various aspects of the spatial modal filter, and design formulas are developed. The note is concluded with a summary in Section VI.

II. DEPARTURE FROM THE IDEAL TEM BEHAVIOR

This class of EMP simulators operating in a pulsed mode is a complex electromagnetic structure to analyze. The complexity is partially due to the fact that the input pulse contains a wide range of frequencies and, consequently, the relevant dimensions of the structure ranges from a small fraction of a wavelength to many wavelengths. Because of this, the simulator while operating in a pulsed mode is a transmission line, a radiator and an optical diffracting structure, all for the same pulse. In reference [15], the electromagnetic characteristics of the simulator were qualitatively discussed by categorizing the frequency range of interest into a) low frequencies, b) high-frequency asymptotics, and c) intermediate frequencies.

At low frequencies, one has near-ideal conditions in terms of simulation because quasi-static considerations apply and the TEM mode of propagation is dominant. The main problem here is to minimize the impedance discontinuity and TEM field discontinuity across the junction between the cylindrical and the conical transmission lines. Such a matching of the TEM modes at the input and output "bends" is achieved by reducing the dispersion distance [12,13].

At higher frequencies, the relevant dimensions of the simulator, e.g., width and spacing of the plate become several wavelengths long, and ray-optical considerations apply. Several canonical problems have been defined and solved [16-19], which are useful in estimating the early-time pulsed fields associated with conducting wedges and thus reduce waveform distortion. Some experimentally measured data [20] is available concerning the early-time fields indicating the $(1/r)$ variation of the spherical

wave launched by the conical line followed by edge diffraction and specular reflections. Some of the problems here are large dispersion times, edge diffractions and excessive ripple in the measured data.

However, it is the intermediate frequencies that present the most serious problems. Relevant distances now become comparable to wavelengths rendering both the quasi-static and the ray-optic considerations inapplicable. In this note, we focus our attention on the behavior of the simulated electromagnetic fields in this frequency regime by taking a superposition of the TEM and non-TEM modes. The non-TEM modes are those supported in a finitely wide two-parallel-plate open waveguiding structure, which are to be contrasted with the familiar propagating modes of a closed rectangular waveguide or a closed circular coaxial transmission line. By taking this view, one can define the problem to be that of damping or suppressing the non-TEM modes without significantly disturbing the desired TEM mode of propagation.

A typical geometry of this class of EMP simulator is shown in Figure 2.1. This figure shows a vertically polarized parallel-plate transmission-line type of simulator. By virtue of symmetry and practicality, it suffices to construct the symmetric half of the structure above the horizontal symmetry plane where a wide conducting plane is placed. Accordingly, Figure 2.1 shows the side view of the simulator comprising the top plate of width $2a$ at a height b above the ground plane. The plate-to-plate separation (for a symmetric situation with two identical parallel plates) is then $2b$ and the lengths of the conical and the parallel-plate transmission lines are designated L and w respectively. With reference to this figure, the nonzero components of electric and magnetic fields for the various modes of propagation in the parallel-plate transmission-line region are:

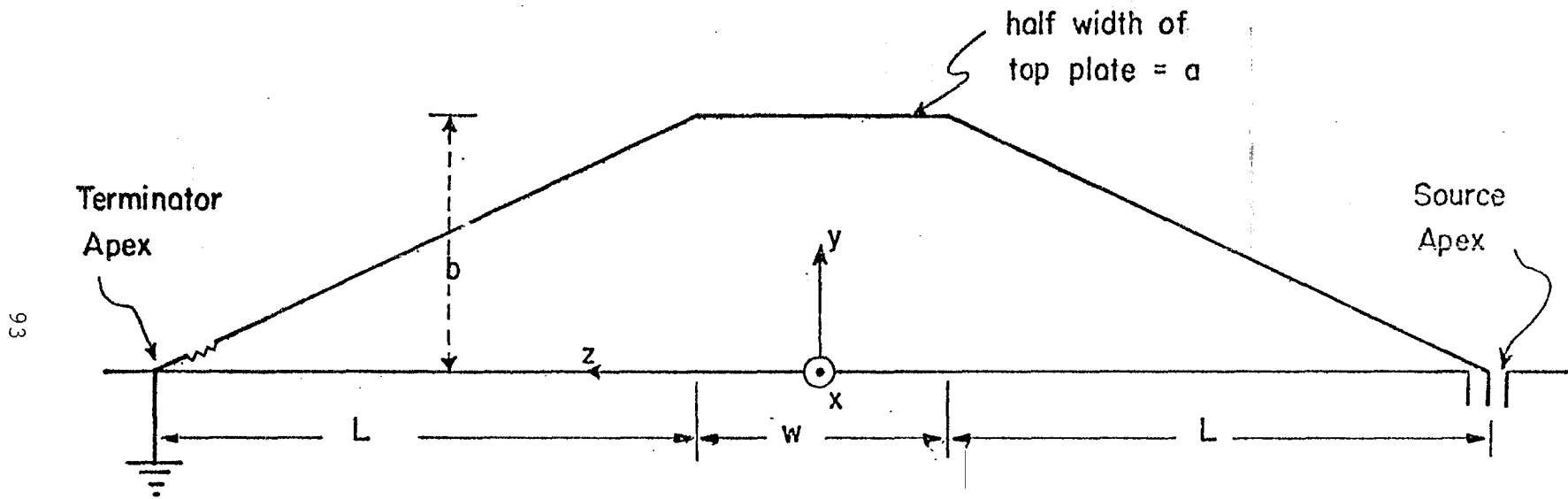


Figure 2.1 Geometry of a vertically polarized, two-parallel plate transmission-line type of EMP simulator

a) TEM mode

$$\tilde{E}_x, \tilde{E}_y, \tilde{H}_x, \tilde{H}_y \quad \text{with} \quad \tilde{E}_z = \tilde{H}_z = 0$$

b) TM mode (E mode)

$$\tilde{E}_z, \tilde{E}_x, \tilde{E}_y, \tilde{H}_x, \tilde{H}_y \quad \text{with} \quad \tilde{H}_z = 0$$

c) TE mode (H mode)

$$\tilde{H}_z, \tilde{H}_x, \tilde{H}_y, \tilde{E}_x, \tilde{E}_y \quad \text{with} \quad \tilde{E}_z = 0$$

All of the above field quantities are functions of position in the transverse plane and frequency. We shall now summarize certain measurements made in the ALECS facility that are relevant in terms of identifying the departure from the ideal TEM behavior. CW measurements [21] made in the working volume of the ALECS facility have detected what has been referred to as the "notch problem". Specifically, the transfer function from the input voltage to the measured fields, when appropriately normalized and plotted as a function of frequency, displays significant notches at certain frequencies. For example, Figure 2.2 shows the magnitude of the normalized transverse magnetic field H_x measured at the center (0,0,0) and the notch is seen to appear at ~25 MHz, with roughly a $\pm 30\%$ ripple at higher frequencies. Figure 2.3 is the normalized principal electric field E_y measured at the same location. It is noted that the principal electric field does not display a notch behavior at the same location, but perhaps a small enhancement. Correspondingly, the experimental measurements in the scale model simulator at Harvard University have reproduced the notch behavior in the field quantities. The description of the experimental setup along with the measured fields

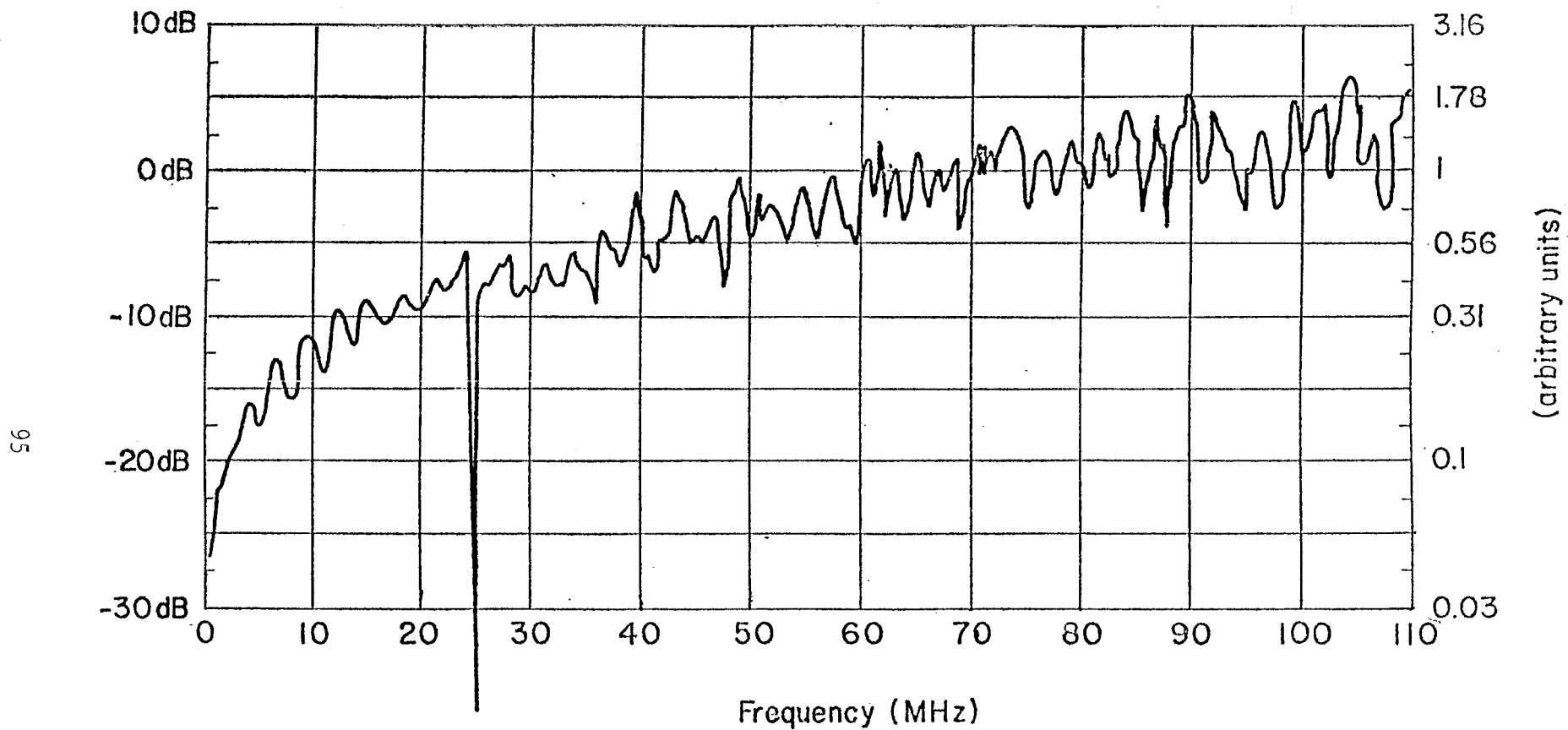
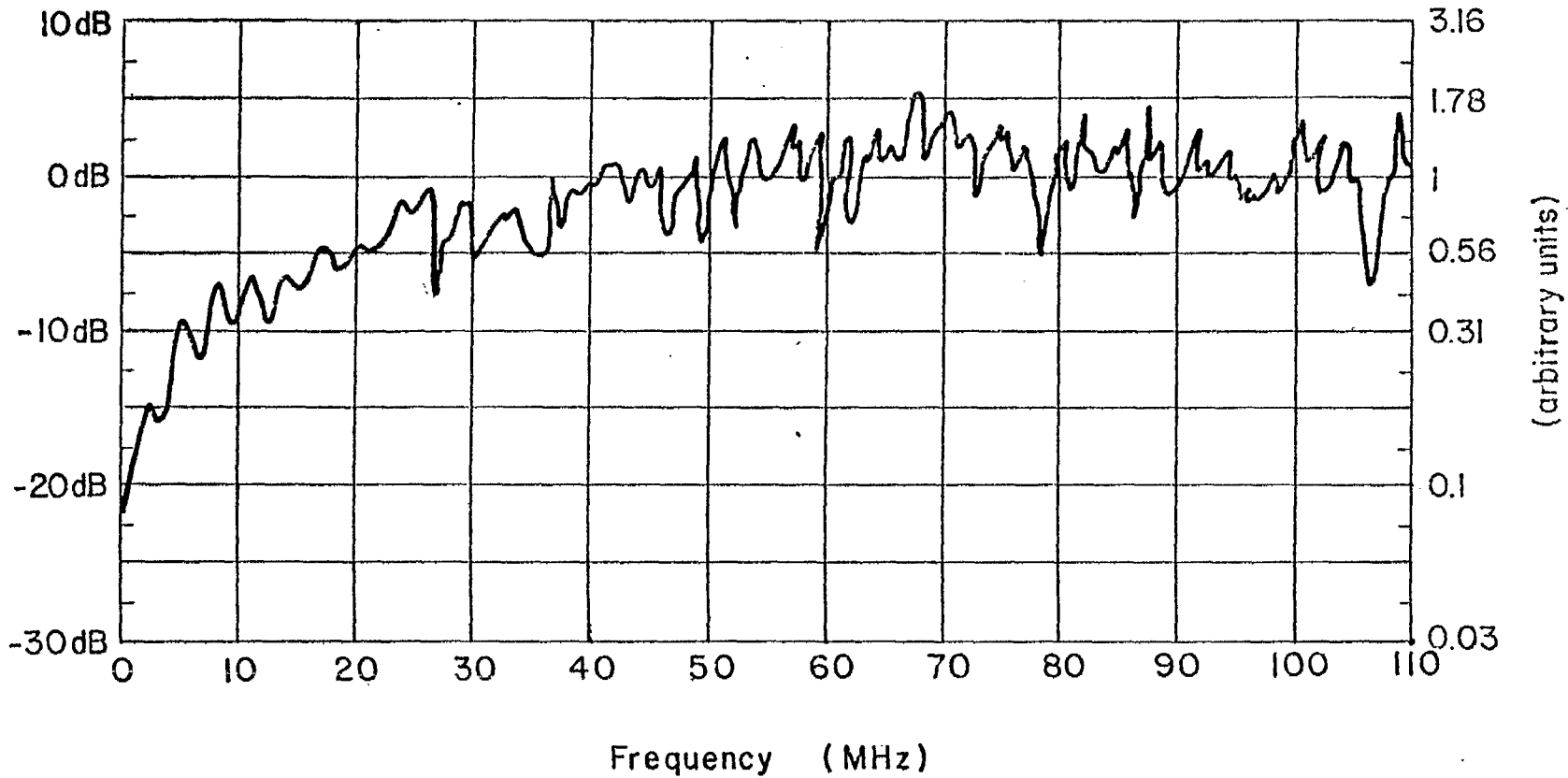


Figure 2.2 Measured $|\dot{B}_x/\text{constant}|$ at the center with coordinates $(0,0,0)$ in ALECS facility

(This figure is reproduced here from reference [21].)



96

Figure 2.3. Measured $|\dot{D}_y/\text{constant}|$ at the center with coordinates (0,0,0) in ALECS facility (This figure is reproduced here from reference [21].)

in the model simulator are well documented in references [22] and [23]. A preliminary measurement of the transverse magnetic field as a function of frequency at a fixed location of (0,0,0) was provided by Blejer [24] and is shown in Figure 2.4. This measurement also displays a sharp null in the magnetic field at ~264 MHz at the measurement location. The null is caused by a cancellation of the transverse magnetic field of the principal TEM mode by that of the first higher TM mode, and the frequency of 264 MHz on the model simulator corresponds very closely to the ~25 MHz notch observed in the ALECS facility. Furthermore, in both configurations (ALECS and the model simulator), the frequencies where one would expect a higher order mode to be excited corresponds approximately to the relevant dispersion distance "d" becoming equal to a half wavelength. Considering a direct path from source apex to load apex and another signal path along the edge of the top plate, d is given by

$$d = \frac{\lambda}{2} \approx 2 \left[\sqrt{b^2 + a^2 + L^2} - L \right] \quad (2.1)$$

where λ is the wavelength corresponding to a frequency where one may expect a higher order TM mode excitation, and the other variables in Eq. (2.1) are illustrated in Figure 2.1. Substituting the values for the various dimensions, we find that the frequency of expected excitation of higher TM mode is ~25 MHz for ALECS and ~256 MHz for the model simulator at Harvard. These compare well with the experimentally observed values of ~24 MHz for ALECS and ~264 MHz for the model simulator. It can be argued that the notch is due to the superposition of the TEM mode and higher order TM and TE modes. The non-TEM

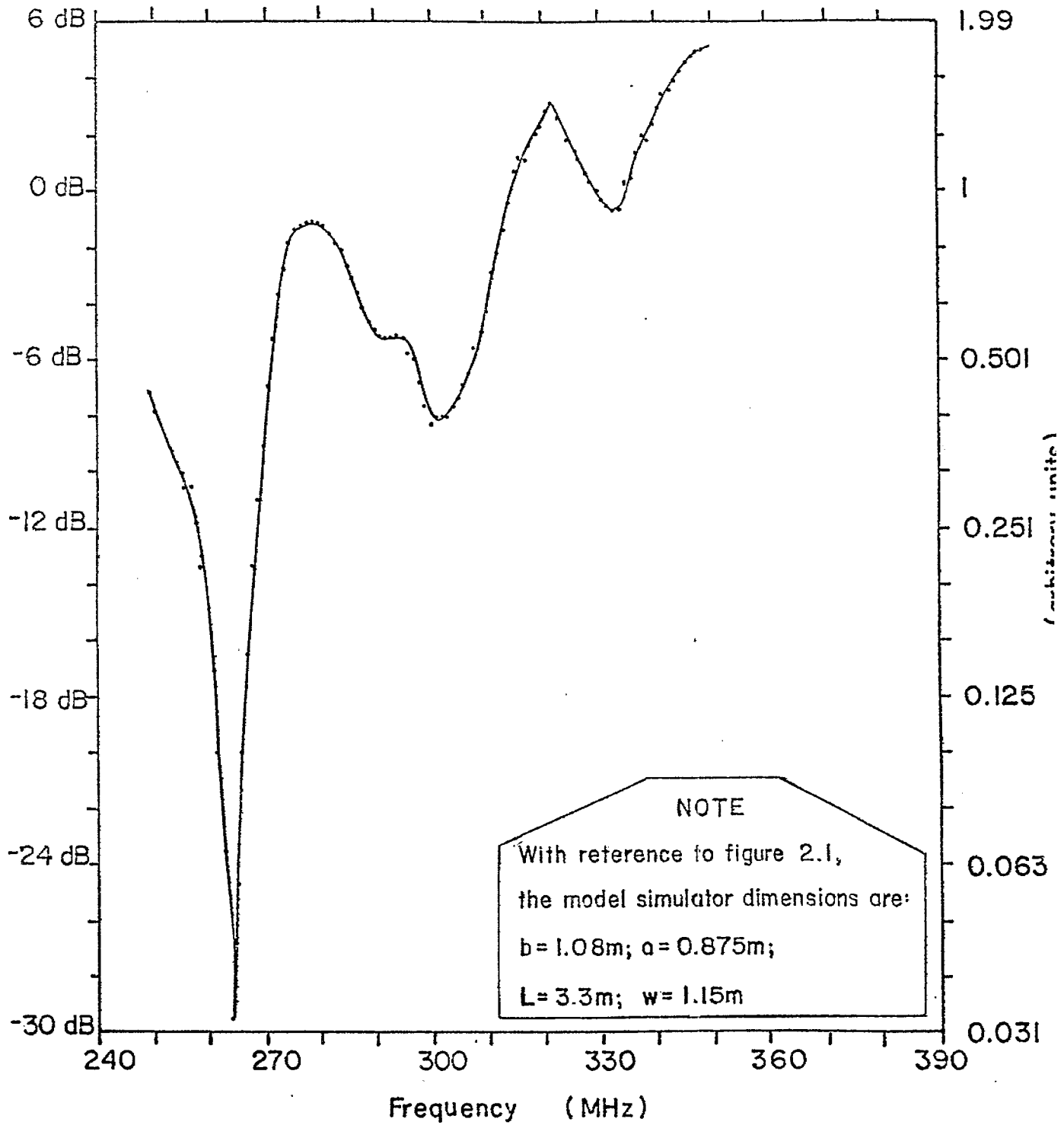


Figure 2.4. Measured $|\dot{B}_x/\text{constant}|$ at (0,0,0) in the model simulator at Harvard [24]

modes being evanescent at either end of the simulator, as expected, all of the input impedance measurements are dominated by the principal TEM mode. Based on these observations, one may conclude that the notch occurs at the center $(0,0,0)$ due to the symmetry in the simulator as a result of near cancellation of the magnetic field of the TEM mode with its counterpart in the first TM mode. We do not expect a near cancellation in the electric field at the same location for the following reasons. The dominant TEM mode is a traveling wave because of the notched load at the end whereas the TE and TM modes are standing waves owing to reflections. The magnetic field (H_x component) in the TM modes propagating in the positive and negative z directions add and their sum cancels the H_x of the principal TEM mode resulting in the notch behavior. However the electric field in the TM modes propagating in the positive and negative z directions cancel from each other and thus one does not expect a notch at $(0,0,0)$ in the electric field. This is consistent with the experimentally measured electric field (E_y) data shown in Figure 2.3. Furthermore, near the top plate both H_x and E_y in the TM mode will have the reversed sign from their values at the ground plane, leading to no cancellation in either of these field quantities with their counterparts in the TEM mode. We also note that the frequency where the notch occurs is also predictable from the dispersion times/distances calculations.

III. CHARACTERISTICS OF NON-TEM MODES

An open waveguide formed by two perfectly conducting parallel plates of finite width can support, in addition to the dominant TEM mode, higher-order TE and TM modes. These higher modes have suitably complex propagation constants which account for the radiation loss of the modes. Because of radiation, power flow and stored energy are not confined to the inner region of the structure. As the wave (a superposition of modal distributions) propagates, there is a continuous "leaking" of energy from the open waveguiding structure.

In closed waveguides, the higher modes are the solutions of source-free time-harmonic Maxwell's equations characterized by axial field variation of the form $\exp[j(\omega t - z k_z)]$. Each one of these modes with real propagation constants (k_z) below cutoff satisfies all of the boundary conditions. Above cutoff k_z is pure imaginary and the modes are evanescent. Also, these modes possess finite energies in a cross section and display orthogonality and completeness properties.

In contrast, the modes on an open waveguide form a discrete spectrum of leaky modes satisfying Maxwell's equations and boundary conditions. However, any cross section extends to infinity and the fields can grow without bounds at large distances from the simulator cross section. These leaky modes on open waveguides do not form a complete orthogonal set and have to be supplemented by a continuous spectrum. The variation of an arbitrary mode can be separated into transverse and longitudinal parts as follows:

$$\tilde{F}(x, y, z, s) = \tilde{f}(x, y, s) e^{-\zeta z} \quad (3.1)$$

where \tilde{F} denotes an arbitrary field component, and \tilde{f} denotes variation in the transverse (x-y) plane. The exponential factor displays axial (z coordinate) variation with ζ (Laplace transformation variable corresponding to the z coordinate) being the longitudinal complex wavenumber. The complex frequency is denoted by s and it is the Laplace transformation variable corresponding to the time t . Setting,

$$p^2 = (s^2/c^2) - \zeta^2 = (\gamma^2 - \zeta^2) \quad (3.2)$$

we have,

$$\zeta = \pm \sqrt{\gamma^2 - p^2} \quad (3.3)$$

To exhibit the cutoff behavior, consider $s = j\omega$, $\gamma = jk$ and $\zeta = jk_z$

$$\zeta = jk_z = \pm \sqrt{(jk)^2 + (\pm jp)^2} = \pm j \sqrt{k^2 + p^2} \quad (3.4)$$

or,
$$k_z = \pm \sqrt{k^2 + p^2} = (\beta + j\alpha) \quad (3.5)$$

In the integral equation formulation [1], complex p , multiplied by a factor with linear dimension appears in the argument of special functions. In order to compute the various field quantities, one looks for the roots of transcendental complex functions of p in the p -plane. These functions are obtainable in closed form for the limiting cases of narrow and wide plates. Denoting a typical root by $p_{n,m}$, the corresponding longitudinal complex wavenumber for this arbitrary mode becomes

$$k_{z_{n,m}} = \pm \sqrt{k^2 + p_{n,m}^2} = \beta_{n,m} + j \alpha_{n,m} \quad (3.6)$$

$p_{n,m}$ values of interest are approximately pure imaginary with relatively small negative real parts. Let

$$p_{n,m} = u_{n,m} + j v_{n,m} ; \quad (|u_{n,m}| \ll |v_{n,m}|)$$

so that

$$k_{z_{n,m}} = \pm \sqrt{(k^2 + u_{n,m}^2 - v_{n,m}^2) + 2j u_{n,m} v_{n,m}} \quad (3.7)$$

If $p_{n,m}$ was pure imaginary (i.e., $u_{n,m} = 0$), the cutoff behavior is easily exhibited by the factor $\pm \sqrt{k^2 - v_{n,m}^2}$. Non-TEM modes are not supported when v exceeds k and k_z becomes pure negative imaginary in the exponential factor, $\exp(-jk_z z)$, and the modes are evanescent. The cutoff behavior for the special case when $[s=j\omega, \gamma=jk$ and $p_{n,m}=j v_{nm}]$ can be summarized as follows. For these special conditions, the longitudinal wavenumber k_z is given by

$$k_{z_{n,m}} = \begin{cases} \beta_{n,m}; & [\text{with } \beta_{n,m} > 0 \text{ and } \alpha_{n,m} = 0] \text{ for propagation} \\ \beta_{n,m} + j\alpha_{n,m}; & [\text{with } \beta_{n,m} > 0 \text{ and } \alpha_{n,m} < 0] \text{ for evanescence} \end{cases} \quad (3.8)$$

Correspondingly, the longitudinal variation of the fields $\exp(-jk_{z_{n,m}} z)$ exhibits the transition from propagation into evanescence. However, the complex singularities ($p_{n,m}$) do have small negative real parts and the transition near cutoff is less abrupt. In the regime of evanescence, the longitudinal wavenumber $k_{z_{n,m}}$ becomes largely pure imaginary with a small real part. Consequently, the exponential longitudinal variation $\exp(-jk_{z_{n,m}} z)$ exhibits evanescence.

Furthermore, a waveguiding structure formed by two finitely wide plates has two planes ($x=0$ and $y=0$) about

which the fields can be symmetric or antisymmetric [25]. Such symmetry decomposition can symbolically be represented by indexing the p-plane singularities as

$$p_{n,m}^{(\pm, \pm, E \text{ or } H)}$$

where n, m correspond to the field variations in x and y directions. The two \pm signs in the superscript indicate symmetry or antisymmetry along the transverse x and y directions and E or H denote TM or TE mode. Thus, such a representation of the p-plane singularities uniquely specifies a mode and its symmetry properties. Consistent with the above notation, the modes themselves can be denoted by $E_{n,m}^{(\pm, \pm)}$ (or $TM_{n,m}^{(\pm, \pm)}$) and $H_{n,m}^{(\pm, \pm)}$ (or $TE_{n,m}^{(\pm, \pm)}$).

These modes in open waveguides formed by a pair of finitely wide parallel plates are found by formulating two different scalar integral equations (of the first kind) for the current and charge densities on the plate. Under certain approximations (separation \gg width or vice versa), the integral equations can be solved analytically by first transforming them into a Fredholm integral equation of the second kind [1,4,5] and using perturbation techniques.

It is not our intention to show detailed modal distributions of these higher modes in this section, but to point out the methods employed and availability of field plots. Specific calculations of the TM modes in a geometry corresponding to the model EMP simulator at Harvard are currently in progress for later comparisons with the measured data. Such comparisons are expected to lead to unambiguous identification of modes.

IV. ELECTROMAGNETIC CONSIDERATIONS OF SPATIAL MODAL FILTERS

The object of introducing a spatial modal filter is to load or damp the non-TEM modes (i.e., TE, TM) without significantly disturbing the TEM modes. One method that has been experimentally implemented in the context of TEM cells [26] with some degree of success is by inserting RF-absorbing material [27,28] along the conducting walls of the waveguiding structure. This technique lacks an analytical basis and also does not fully exploit the uniform characteristics of the dominant TEM mode for damping the non-TEM modes. If we recognize the fact that all propagating modes have spatial properties, one can, hence, take advantage of certain spatial properties to selectively load the modes [29]. In a two-parallel-plate transmission-line type of EMP simulator, all of the important characteristics of the principal TEM mode, both in the parallel-plate region [9] and the conical plate region [10,11], are well known and documented. The quantities of interest are the characteristic impedance, equipotential and field distributions, and field uniformity. Later in this section we shall use a knowledge of these quantities in developing a spatial modal filter. Such filters can take various forms and we dimensionally categorize them below:

A. Zero Dimensional

A zero dimensional spatial modal filter will essentially act like a directional coupler in a transmission line that couples to backward propagating modes. In the case of a simulator under consideration, this type of SMF can take the form of two receiving or parasitic antennas (equivalent dipoles, loops) suitably oriented on the top plate or the ground plane so that the TEM mode is uncoupled. The sensitivity of damping of the non-TEM modes is governed by local field ratios.

B. One Dimensional

One-dimensional spatial modal filters can be implemented by having longitudinal slots both in the top plate and the ground plane. The longitudinal slots (directed along the z-axis of Figure 2.1 in the parallel-plate region and directed along the spherical radial coordinate in the conical region) will be resistively loaded by transverse resistors (x-direction in Figure 2.1). By definition, the only mode with longitudinal component of magnetic field (H_z) is the TE mode and, hence, this mode has principally transverse currents (J_x) which couple to the transverse resistors. Consequently, this form of SMF is essentially uncoupled from the principal TEM or higher TM modes while loading the higher TE modes.

C. Two Dimensional

An extension of the one-dimensional SMF is to introduce "loading sheets" that are comprised of a two-dimensional (transverse and longitudinal) array of resistors. In the top plate and the ground plane, one would have only transverse resistors, but in the space away from the simulator plates, the loading sheet will be two dimensional. The sheet will be located along an equipotential surface of the principal TEM mode. This implies that the sheet is electromagnetically invisible to the principal TEM mode while coupling and, hence, damping the non-TEM modes.

D. Three Dimensional

The two-dimensional loading sheet described above can be repeated to fill some portion of the volume between the top plate and the ground plane resulting in a volumetric suppressor of non-TEM modes.

There are certain constraints to be placed on the choice of the volume of space wherein such a filter can be

placed. For example, the filter should not be close to the working volume of the simulator to avoid any coupling to the test object. Furthermore, the higher-order TE and TM modes become evanescent at a certain distance away from the terminator in the output section. For this reason, little is gained by placing the volumetric SMF near the termination. Such considerations indicate that the SMF should be placed under the output bend extending toward, but not close to, the terminator.

In Section V, we develop an approximate analytical basis for estimating the sheet resistors.

V. ESTIMATION OF SHEET IMPEDANCES

In this section, we derive relations useful in estimating the longitudinal and transverse resistor values in the individual sheets of a volumetric suppressor. A cross-sectional view of the SMF is sketched in Figure 5.1. Essentially the mode filter would consist of several layers of resistor arrangement, wherein each layer consists of a two-dimensional array of resistors along the axial and transverse directions. Each layer would coincide with a TEM equipotential surface in a conical transmission line. The equipotential and field calculations in a conical transmission line have been reported [10,11], and they are based on stereographically projecting the two-conical-plate line into a cylindrical line of two circular arcs on two different circles. The curved-cylindrical-plate problem is later solved by the method of conformal mapping for the TEM quantities. The physical quantity that is relevant for the SMF design is the TEM equipotential surface, an example of which is shown plotted in Figure 5.2. In this figure, the top plate is held at a potential of V_0 with the ground plane as the reference. The equipotentials (magnetic field lines) are shown in steps of $0.1 V_0$ and the stream lines (electric field lines) in steps of $0.1 U_0$. U_0 is the total current flowing on half of the top plate. The individual resistive sheets of the volumetric suppressor will be made to coincide with the calculated surfaces.

In estimating the values of the transverse (R_t) and the longitudinal (R_l) resistors, it is useful to view the two-dimensional array of resistors on any given equipotential surface as a resistive sheet with an impedance of Z_s . We now consider the following two canonical problems useful in estimating R_l and R_t . The two problems are posed and analyzed by viewing the mode suppressor sheets as plane wave absorbers.

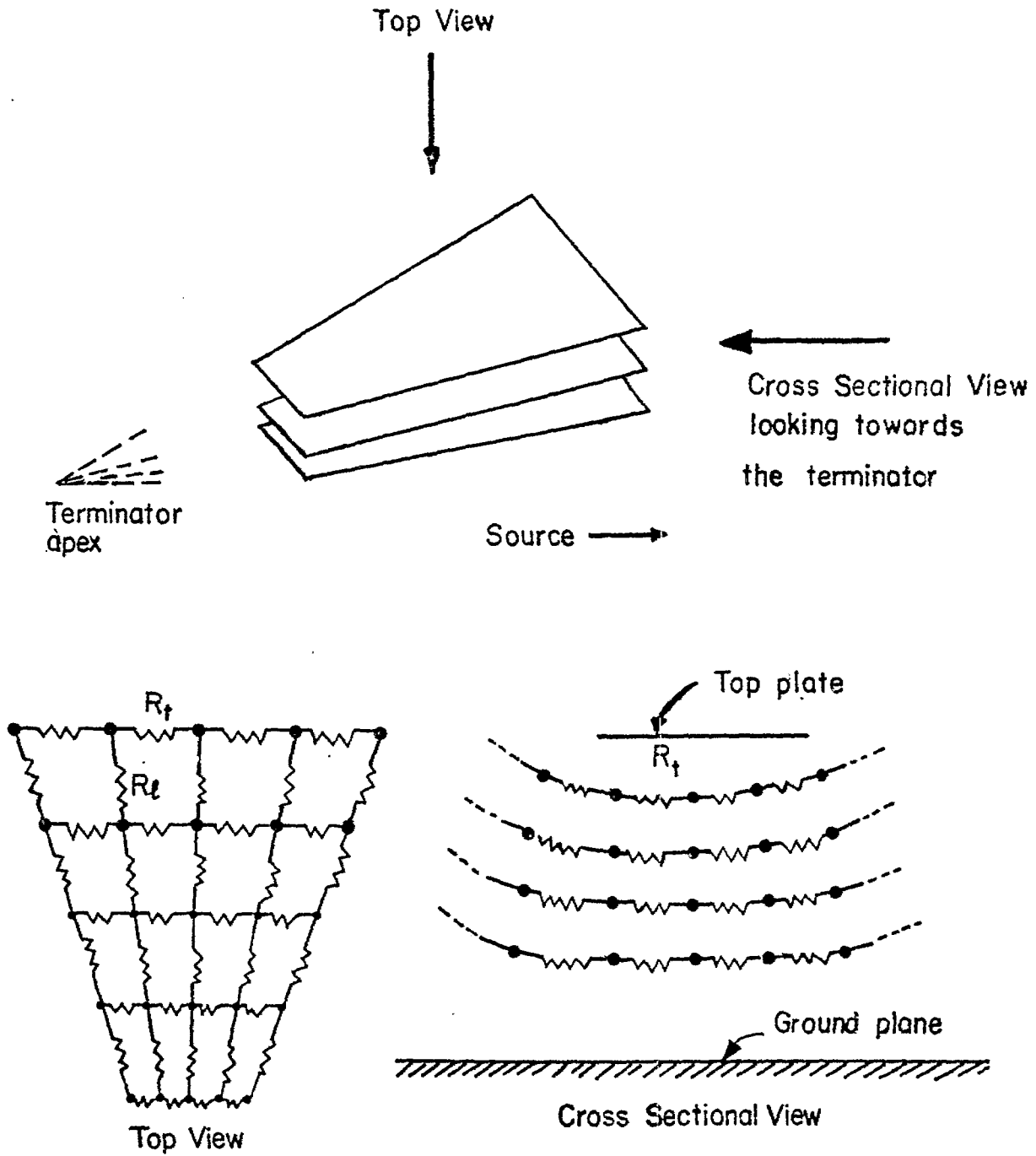


Figure 5.1 Structure of the volumetric spatial modal filter

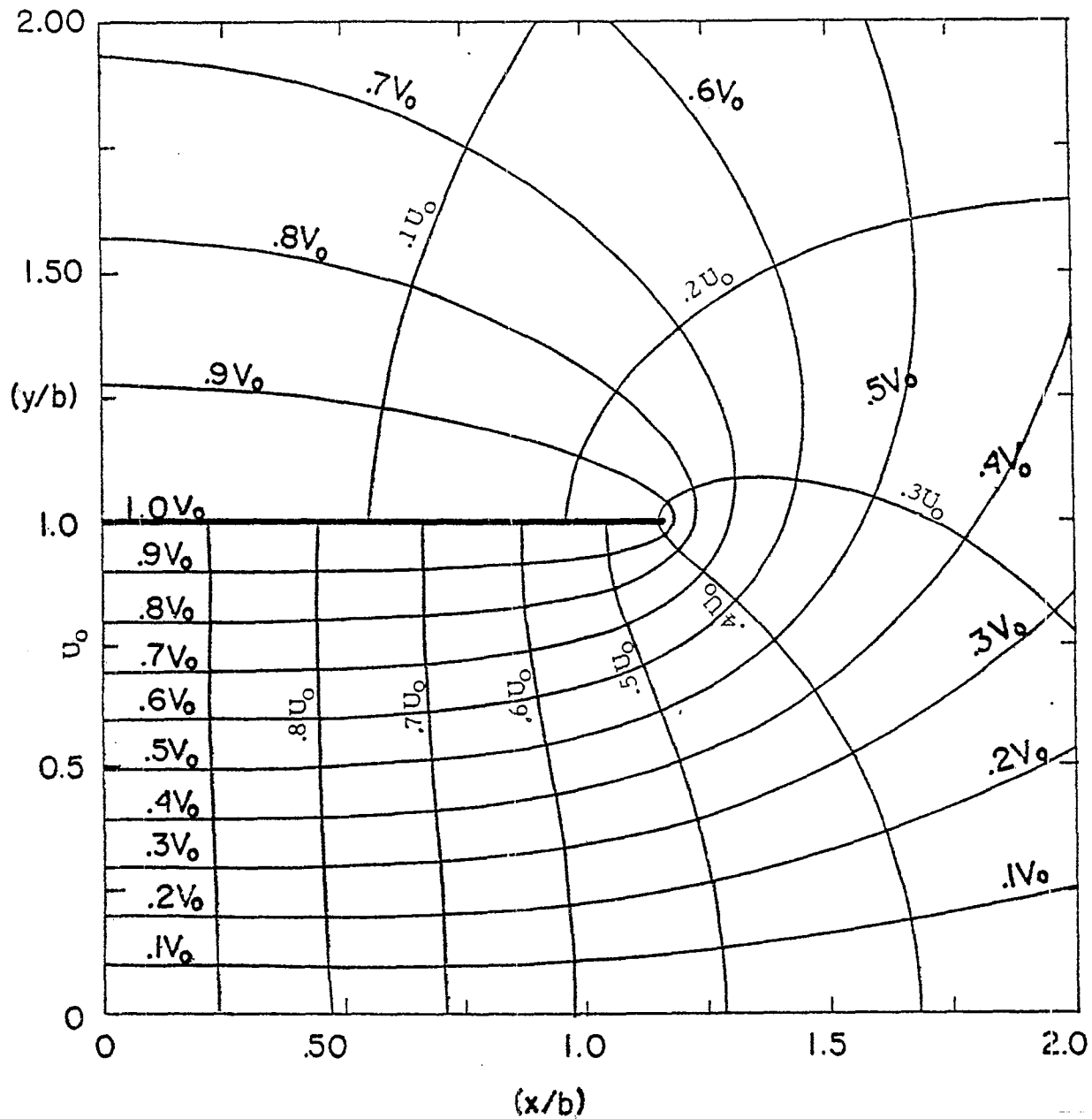


Figure 5.2 A typical TEM equipotential and electric field lines in the conical transmission line [(b/a) = 0.857 and (L/b) = 4.2; scale model simulator with $z_c^{(TEM)} = 82\Omega$ from top plate to ground plane]

A. TM Waves Incident on the Resistive Sheet

Consider a TM wave incident on the resistive sheet (Z_s in Ω), as shown in Figure 5.3a. Denoting the induced surface current density on the sheet by J_s (A/m), the boundary conditions on the tangential components of the electric and magnetic field lead to

$$E_{\text{tan}} = E_i \sin(\alpha) - E_r \sin(\alpha) = E_t \sin(\alpha) \quad (5.1)$$

The difference in the tangential magnetic field is

$$\Delta H_{\text{tan}} = H_{\text{top}} - H_{\text{bottom}} = H_i + H_r - H_t = J_s = E_{\text{tan}}/Z_s \quad (5.2)$$

J_s is positive and is directed from left to right in Figure 5.3a. Note that the free space characteristic impedance Z_0 is given approximately by

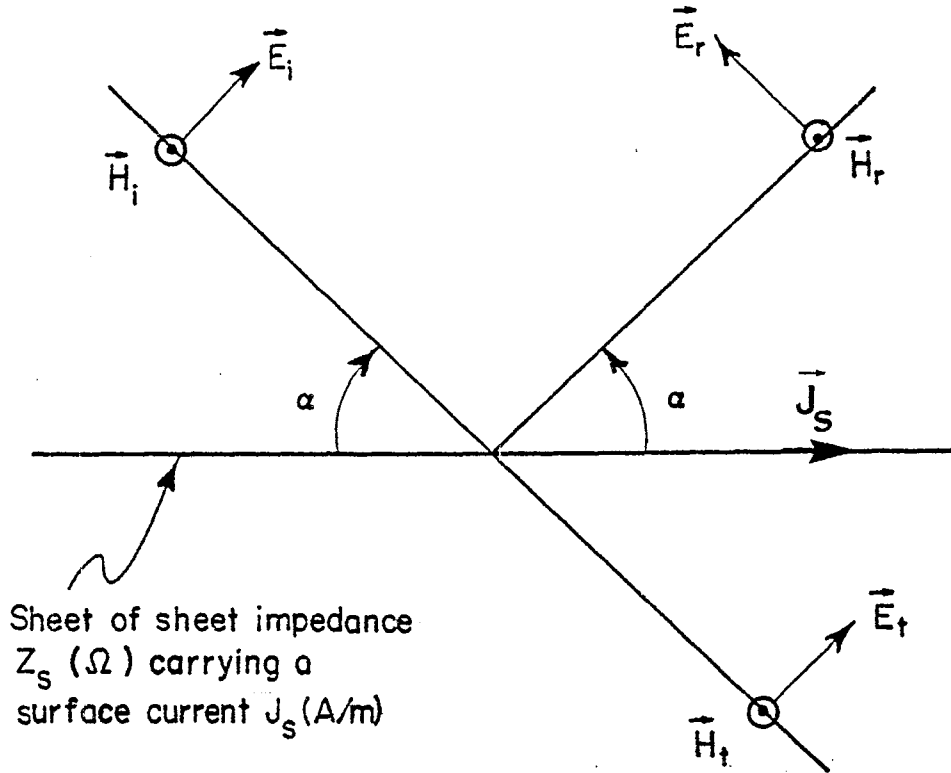
$$Z_0 = \frac{E_i}{H_i} = \frac{E_r}{H_r} = \frac{E_t}{H_t} \approx \sqrt{\frac{\mu_0}{\epsilon_0}} \quad (5.3)$$

Using Eq. (5.3) in Eq. (5.2), and then making use of $E_r = E_i - E_t$ from Eq. (5.1), we can get

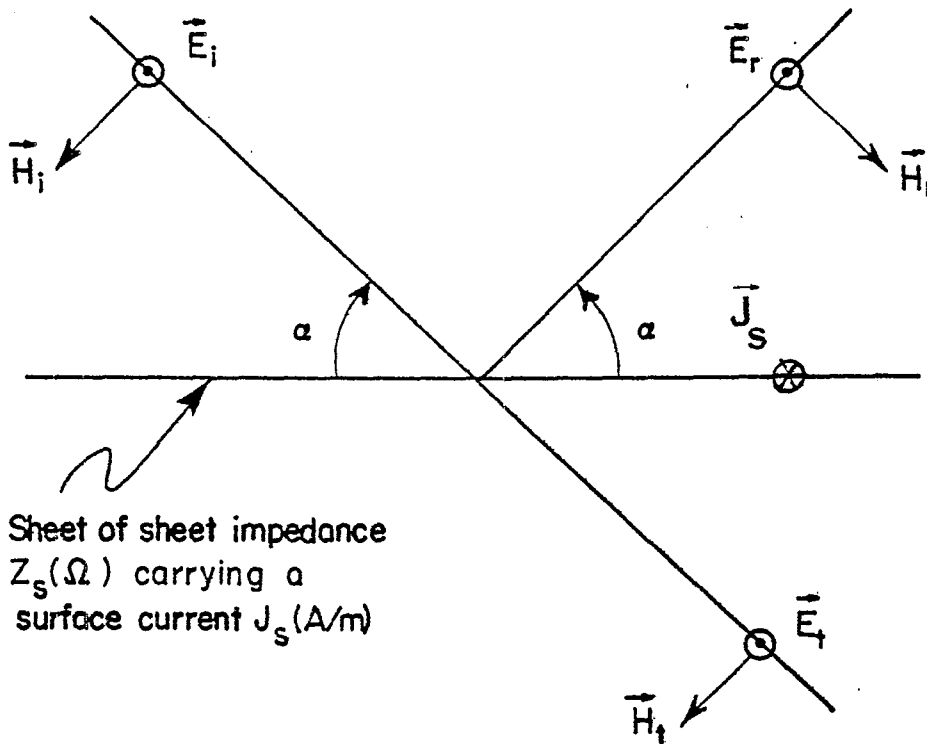
$$\frac{E_t}{E_i} = \frac{2 Z_s}{2 Z_s + Z_0 \sin(\alpha)} \quad (5.4)$$

For fixed values of E_i and α , the power dissipated in the sheet per unit area,

$$\begin{aligned} P &= E_{\text{tan}} J_s = (E_{\text{tan}}^2/Z_s) = (E_t^2 \sin^2(\alpha)/Z_s) \\ &= \frac{E_i^2 \sin^2(\alpha)}{Z_s} \left(\frac{2 Z_s}{2 Z_s + Z_0 \sin(\alpha)} \right)^2 \end{aligned} \quad (5.5)$$



a) TM wave incident on a resistive sheet



b) TE wave incident on a resistive sheet

Figure 5.3 Mode suppressor sheets viewed as plane wave absorbers

Now the power dissipated as heat from the incident wave per unit area normal to the incident wave is

$$P_W = P/\sin(\alpha) = \left(\frac{E_i^2}{Z_0} f \right) \quad (5.6)$$

where f is the fractional power lost, and is given by

$$f = \frac{Z_0}{E_i^2} \frac{P}{\sin(\alpha)} = \frac{Z_0}{Z_s} \sin(\alpha) \left(\frac{2 Z_s}{2 Z_s + Z_0 \sin(\alpha)} \right)^2 \quad (5.7)$$

Setting

$$\eta = \frac{Z_s}{Z_0 \sin(\alpha)} \quad (5.8)$$

we have

$$f = \frac{1}{\eta} \left[\frac{2\eta}{1 + 2\eta} \right] \quad (5.9)$$

We may now maximize the fractional power lost by requiring

$$\frac{df}{d\eta} = 0 \quad ; \quad \text{leading to } \eta_{\text{opt}} = 1/2$$

This give an optimum value for the sheet impedance of

$$Z_s^{(\text{opt})} = \frac{Z_0 \sin(\alpha)}{2} \quad (5.10)$$

Equation (5.10) is now useful in estimating the longitudinal resistors R_ℓ which carry the current for the TM mode of propagation.

B. TE Waves Incident on the Resistive Sheet

We can use an entirely similar analysis as in the TM case for the TE case. Consider a TE wave incident on a resistive sheet of impedance Z_s in Ω at an angle α as shown in Figure 5.3b. Let the induced surface current on the resistive sheet be denoted by J_s (A/m). The boundary conditions on the tangential fields are

$$E_{\text{tan}} = -E_i - E_r = -E_t \quad (5.11)$$

The difference in the tangential magnetic field is

$$\begin{aligned} \Delta H_{\text{tan}} &= H_{\text{top}} - H_{\text{bottom}} = -H_i \sin(\alpha) + H_r \sin(\alpha) + H_t \sin(\alpha) \\ &= J_s = (E_{\text{tan}}/Z_s) \end{aligned} \quad (5.12)$$

J_s is positive and directed into the plane of the paper in Figure 5.3b. As before, using Eq. (5.3) in (5.12) and later using Eq. (5.11), we can get

$$\frac{E_t}{E_i} = \frac{2 Z_s \sin(\alpha)}{2 Z_s \sin(\alpha) + Z_0} \quad (5.13)$$

Once again, the power dissipated in the sheet per unit area is

$$\begin{aligned} P &= E_{\text{tan}} J_s = (E_{\text{tan}}^2/Z_s) = (E_t^2/Z_s) \\ &= \frac{E_i^2}{Z_s} \left(\frac{2 Z_s \sin(\alpha)}{2 Z_s \sin(\alpha) + Z_0} \right)^2 \end{aligned} \quad (5.14)$$

Using Eq. (5.6), the fractional power lost is now given by

$$f = \frac{Z_o}{E_i^2} \frac{P}{\sin(\alpha)} = \frac{Z_o}{Z_s \sin(\alpha)} \left(\frac{2 Z_s \sin(\alpha)}{2 Z_s \sin(\alpha) + Z_o} \right)^2 \quad (5.15)$$

$$= \frac{1}{v} \left[\frac{2v}{1 + 2v} \right] \quad (5.16)$$

where $v = (Z_s \sin(\alpha)/Z_o)$. We may now maximize the dissipated power by requiring

$$\frac{df}{dv} = 0 \quad ; \quad \text{leading to } v_{\text{opt}} = 1/2 \quad (5.17)$$

This gives an optimum value for the sheet impedance of

$$Z_s^{(\text{opt})} \approx \frac{Z_o}{2 \sin(\alpha)} \quad (5.18)$$

Once again, we note that for the TE case, only the transverse resistors carry current and, hence, Eq. (5.18) applies to the transverse resistors R_t .

In either case of TM or TE waves incident on the resistive sheets, the values of the resistors R_ℓ and R_t are dependent on the angle of incidence of these waves onto the sheets. In a simulator configuration, this angle (α) is, of course, a variable quantity and, consequently, an experimental optimization of the particular values of the resistors is inevitable.

However, at high frequencies, where ray-optic considerations apply, one can estimate the angle α by considering a typical ray path. It is estimated that the present high frequency ripple of $\pm 30\%$ can be reduced to within $\pm 10\%$. At intermediate frequencies, the angles are harder to estimate, but effective removal of energy from the non-TEM modes results from multiple passes. It is likely that for E modes (TM case), the ratio of E_z to E_x or E_y may define an effective angle α . A future memo will address these issues specifically.

For the experimental evaluation, initially, a typical angle may be chosen in designing the filter and, later, experimentation around these values will determine the final values.

In successfully implementing these concepts in a given experimental situation, there will be several associated problems and considerations unique to the experiment. For instance, in a model simulator experiment, the power levels are low and, hence, energy dissipation in the resistors is not a serious consideration. However, on a full-scale facility (e.g., ALECS), it may become necessary to place the resistors in plastic tubes filled with oil (if required). Also, in an on-site configuration, the mechanical problems of supporting and holding the sheet along equipotential contours are much more severe. There are questions like how far outward in the cross section should the sheets extend. Such considerations and a detailed design, fabrication and evaluation of the proposed volumetric suppressor will form the subject of a separate report.

VII. SUMMARY

A two-parallel-plate transmission-line type of EMP simulator has been historically employed to propagate an electromagnetic pulse with a plane wavefront. Since the pulse consists of a wide frequency spectrum, the structures that have been built propagate modes other than the principal TEM mode. Consequently, techniques of non-TEM mode suppression is an important element in the advancement of simulator technology. In this note, we address the problem of mode suppression and, in particular, the electromagnetic considerations of a volumetric suppressor. This suppressor is the result of one of several techniques of mode suppression and believed to be the most efficient. Empirical relations are developed for computing the resistor values required in the fabrication by viewing the suppressor as a plane wave absorber.

An important feature of the SMF is its location. Figure 6.1 shows the side view of a parallel-plate EMP simulator, indicating the approximate locations of two possible SMF. The SMFs have to be located away from the two apexes where the non-TEM modes are evanescent. It is also essential to place the SMF so as to minimize any coupling effects with the test object.

Finally, although our present interest is in EMP simulators, it is recognized that the mode suppression considerations presented here are fairly general and can apply to other types of multimoded structures (e.g., TEM cell) where the non-TEM modes are also undesirable, and due to the lack of radiation losses can cause even more severe problems.

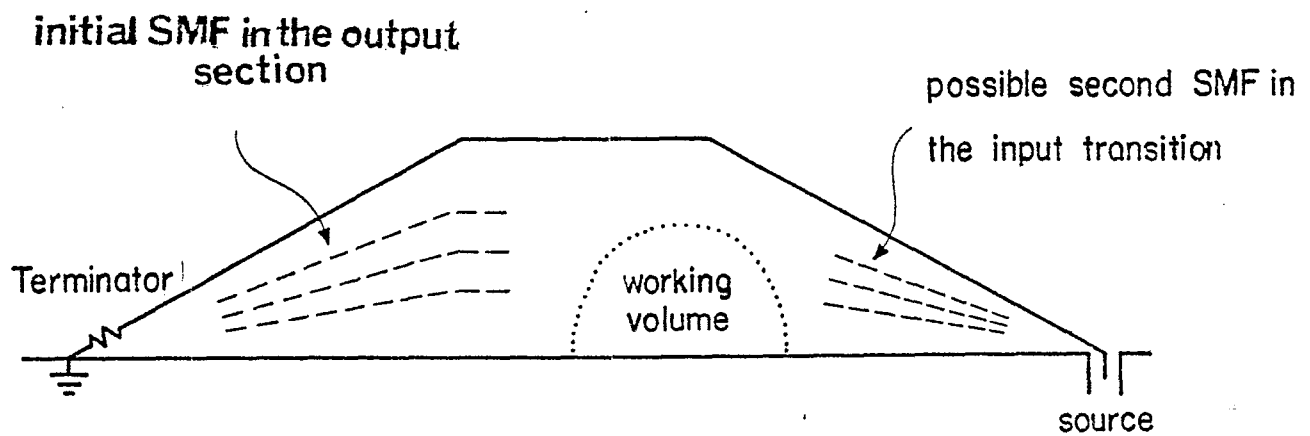


Figure 6.1 Side view of the simulator showing the approximate locations of two possible spatial modal filters (SMF)

REFERENCES

1. L. Marin, "Modes on a Finite-Width, Parallel Plate Simulator: I. Narrow Plates", Sensor and Simulation Note 201, September 1974.
2. C-M. Chu, "Mathematics of Guided Wave Propagation in Open Structures", Sensor and Simulation Note 206, May 1974.
3. T. Itoh and R. Mittra, "Analysis of Modes in a Finite Width Parallel-Plate Waveguide", Sensor and Simulation Note 208, January 1975.
4. L. Marin, "Modes on a Finite-Width, Parallel-Plate Simulator: II. Wide Plates", Sensor and Simulation Note 223, March 1977.
5. L. Marin and G.C. Lewis, "Modes on a Finite-Width Parallel-Plate Simulator: III. Numerical Results for Modes on Wide Plates", Sensor and Simulation Note 227, September 1977.
6. A.E.H. Love, "Some Electrostatic Distributions in Two Dimensions", Proc. London Math. Soc., Vol. 22, pp. 337-369, 1923.
7. C.E. Baum, "Impedance and Field Distributions for Parallel Plate Transmission Line Simulators", Sensor and Simulation Note 21, June 1966.
8. T.L. Brown and K.D. Granzow, "A Parameter Study of Two-Parallel-Plate Transmission Line Simulators of EMP Sensor and Simulation Note 21", Sensor and Simulation Note 52, April 1968.
9. C.E. Baum, D.V. Giri and R.D. González, "Electromagnetic Field Distribution of the TEM Mode in a Symmetrical Two-Parallel-Plate Transmission Line", Sensor and Simulation Note 219, 1 April 1976.
10. F.C. Yang and K.S.H. Lee, "Impedance of a Two-Conical-Plate Transmission Line", Sensor and Simulation Note 221, November 1976.
11. F.C. Yang and L. Marin, "Field Distributions on a Two-Conical-Plate and a Curved Cylindrical-Plate Transmission Line", Sensor and Simulation Note 229, September 1977.

12. C.E. Baum, "The Conical Transmission Line as a Wave Launcher and Terminator for a Cylindrical Transmission Line", Sensor and Simulation Note 31, January 1967.
13. C.E. Baum, "General Principles for the Design of ATLAS I and II, Part V: Some Approximate Figures of Merit for Computing the Waveforms Launched by Imperfect Pulser Arrays onto TEM Transmission Lines", Sensor and Simulation Note 148, 9 May 1972.
14. K.S.H. Lee, of Dikewood Industries, Inc., private communication, October 1978.
15. D.V. Giri, C.E. Baum, R.W.P. King, D.J. Blejer and S-K. Wan, "Experimental Investigations into Higher-Order Mode Effects and Simulator/Object Interaction in Parallel-Plate Transmission-Line Geometries", Miscellaneous Simulator Memo 11, 26 May 1977.
16. C.E. Baum, "The Diffraction of an Electromagnetic Plane Wave at a Bend in a Perfectly Conducting Planar Sheet", Sensor and Simulation Note 47, 9 August 1967.
17. J.B. Keller and A. Blank, "Diffraction and Reflection of Pulses by Wedges and Corners", Comm. on Pure and Applied Math., Vol. 4, p. 75, 1951.
18. D.F. Higgins, "The Diffraction of an Electromagnetic Plane Wave by Interior and Exterior Bends in a Perfectly Conducting Sheet", Sensor and Simulation Note 128, January 1971.
19. K.K. Chan, L.B. Felsen, S.T. Peng and J. Shmoys, "Diffraction of the Pulsed Field from an Arbitrarily Oriented Electric or Magnetic Dipole by a Wedge", Sensor and Simulation Note 202, October 1973.
20. D.L. Endsley and D.B. Westenhaver, "Special Report on Field Measurements", ALECS Memo 4, 28 December 1967.
21. J.C. Giles, M.K. Bungardner, G. Seely and J. Furaus, "Evaluation and Improvement of the CW Performance of the ALECS Facility," ALECS Memo 10, Volume I, Technical Discussion, September 1975.
22. T.T. Wu, R.W.P. King, D.J. Blejer and S-K. Wan, "Laboratory Model Parallel-Plate Transmission Line Type of EMP Simulator (Description of the Set-up and Sample Measurements)," Miscellaneous Simulator Memo 16, 31 July 1977.

23. M. Krook, R.W.P. King, D.J. Blejer, T.K. Sarkar and S-K. Wan, "The Electric Field in a Model Parallel-Plate EMP Simulator at a High CW Frequency," Miscellaneous Simulator Memo 17, July 1978.
24. D.J. Blejer of Harvard University, private communication, November 1978.
25. C.E. Baum, "Interaction of Electromagnetic Fields with an Object Which Has an Electromagnetic Symmetry Plane", Interaction Note 63, 3 March 1971.
26. M.L. Crawford, "Generation of Standard EM Fields Using TEM Transmission Cells", IEEE Trans. on Electromagnetic Compatibility, Vol. EMC-16, pp. 189-195, November 1974.
27. M.L. Crawford, J.L. Workman and C.L. Thomas, "Generation of EM Susceptibility Test Fields Using a Large Absorber-Loaded TEM Cell", IEEE Trans. on Instrumentation and Measurement, Vol. IM-26, No. 3, pp. 225-230, September 1977.
28. M.L. Crawford, J.L. Workman and C.L. Thomas, "Expanding the Bandwidth of TEM Cells for EMC Measurements", IEEE Trans. on Electromagnetic Compatibility, Vol. EMC-20, No. 3, pp. 368-375, August 1978.
29. D.V. Giri and C.E. Baum, "Spatial Modal Filters for Suppression of Non-TEM Modes in Parallel Plate Simulators", presented at the Nuclear EMP Meeting held at the University of New Mexico and sponsored by IEEE Albuquerque Joint Chapters (AP-S, MTT-S, EMC-S) and the Department of Electrical Engineering and Computer Science, University of New Mexico, 6-8 June 1978.